Image Processing & Communications, vol. 21, no. 1, pp.1-42
DOI: 10.1515/ipc-2016-0002

OPTIMAL COMBINERS IN PRE-AMPLIFIED OPTICAL WIRELESS SYSTEMS UNDER MEDIUM-TO-STRONG ATMOSPHERIC TURBULENCE

NIKOS C. SAGIAS[1] ANTHONY C. BOUCOUVALAS[1] KOSTAS YIANNOPOULOS[1] MURAT UYSAL[2]
ZABIH GHASSEMLOOY[3]

[1]Department of Informatics and Telecommunications, University of Peloponnese, Tripoli 22131, Greece,
nsagias@ieee.org
[2]Faculty of Engineering, Ozyegin University, Istanbul 34662, Turkey.
[3]Faculty of Engineering and Environment, Northumbria University, Newcastle upon Tyne NE1 8ST, UK.

Abstract. In this work we analytically investigate optimal combiners for pre-amplified diversity receivers that operate under medium-to-strong atmospheric turbulence. We first demonstrate that the combiner performance is strongly affected by the existence of a signal-amplified spontaneous emission beat noise at the output of the photodetector. Due to the signal-dependent nature of noise, the optimal combiner can be classified as a hybrid one, of which performance is between the well-known equal-gain and maximal-ratio combiner architectures. Having established the optimal design, we further assess the proposed combiner performance over gamma-gamma and negative-exponential fading environments.

Key words. Bit-error-rate, outage probability, negative-exponential fading, outdoor optical wireless, optical amplifiers, diversity reception.

1 Introduction

Multi-Gb/s optical wireless communication (OWC) systems constitute a viable, low-cost and truly broadband interconnection alternative for the implementation of data networks with a radius of a few kms. The capacity that is provided by optical technologies, however, can only be fully utilized by properly taking into account the adverse aspects of the optical beam transmission through the atmosphere and compensating for them. The temperature and pressure dependent nature of the atmosphere's refractive index causes transmission effects such as beam wander, spreading and time-varying losses [2] that ultimately manifest as scintillations, i.e., random intensity fluctuations of the optical wave-front. Therefore, the OWC link may suffer an outage when the scintillation becomes severe enough to lower the received power under the required sensitivity. The deleterious impact of atmosphere-induced scintillations on the OWC link performance has been studied in depth in the literature and numerous tech-

niques been proposed with a goal to immunize the OWC system against the stochastic response of the atmospheric channel. Applicable techniques include the focusing of beams by mirrors [7], beam averaging on large aperture receivers [18], diversity in the space and time domains [9, 10, 12, 14, 19], coding [3, 17, 20, 23], relaying [5, 6, 16] and amplification [1, 5, 13, 15]. Combinations of these techniques have also been proposed, while the co-utilization of spatial diversity and amplification has previously reported increased resilience against fades by using optical amplifiers in conjunction with equal-gain combiners (EGCs) at the electronic receiver [15, 22].

Within this context, we have recently demonstrated that a significant link gain can be obtained by deploying optimal combiners in a multi-branch receiver arrangement with amplification [21]. Optimal combiners in amplified systems can be classified as hybrid. Hybrid combiners performance is between EGCs and maximal-ratio combiners (MRCs), due to the existence of a signal-with-optical-noise beating term that dominates the receiver. The beat noise power is signal dependent and this leads to a dual operation of optimal combiners. Specifically, whenever a branch enters a fade state, thus the signal (and the beat noise) power is low, the combiner treats the branch as an MRC and applies a gain that is signal dependent. If the branch signal is strong enough, then the corresponding gain stabilizes so as not to further aggravate the impact of the beat noise, and the combiner treats the branch as an EGC. Our previous study was limited to moderate turbulence and the results presented therein suggested that optimal combiners are better suited for deployment in more adverse conditions, which are typically expected in the saturated turbulence regime. In this work we investigate the optimal combiner performance in both gamma-gamma and negative-exponential fading environments [4], and discuss whether the proposed combiners can indeed attain an additional benefit when compared with other combiner structures.

The rest of this paper has the following structure: in Section 2 we present a basic mathematical model for the description of the OWC channel, the optical amplifier and the multi-branch receiver. Section 3 calculates the outage probability and the average bit error rate (BER) of the selection combiner (SC) and the EGC, as well as the optimal combiner structure. Analytical and simulation results, that quantify the performance evaluation of the proposed optimal combiner, are illustrated in Section 4, where it is also demonstrated that the optimal combiner provides a link gain improvement as compared to MRC and EGC.

2 Channel, Amplifier and Receiver Models

The proposed system is presented in Fig. 1. The OWC signal propagates through the atmosphere and experiences turbulence induced fading. At the receiving side, L identical optical antennas are deployed and the output of each antenna is fed to an optical amplifier. The role of the amplifier is to increase the corresponding branch sensitivity and therefore enhance its resilience against fades. Each amplifier output is applied to a photodetector (PD) and L photocurrent outputs are combined in a linear fashion prior to signal detection.

For the rest of the analysis, we assume that the received optical powers Z_i with $Z_i, i = 1, 2, \ldots, L$ are statistically independent and identically distributed (iid) random variables (RVs). In the medium turbulence regime, the stochastic channel response is accurately described by the γ–γ model, with a probability density function (pdf) that is given by

$$f_{Z_i}(z) = \frac{2\,(m_y\,m_x)^{\frac{m_y+m_x}{2}}}{\Gamma(m_x)\,\Gamma(m_y)} \left(\frac{L}{\overline{P}_{\rm in}}\right)^{\frac{m_y+m_x}{2}} \times z^{\frac{m_y+m_x}{2}-1} K_{m_y-m_x}\left(2\sqrt{m_y\,m_x\,\frac{L\,z}{\overline{P}_{\rm in}}}\right). \quad (1)$$

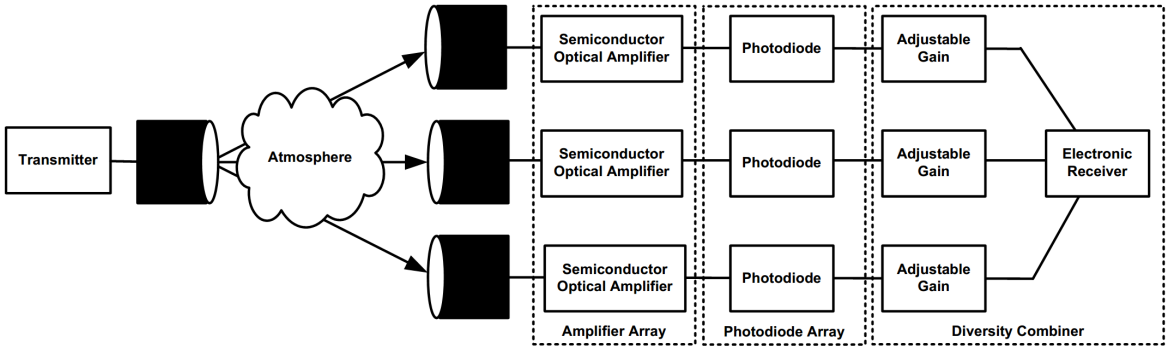

Fig. 1: Optically pre-amplified system with diversity

In the above equation, $\overline{P}_{\text{in}}$ is the total average input optical power at the receiver, while all branches receive an equal amount of optical power on average, $K_v(\cdot)$ and $\Gamma(\cdot)$ denote the modified Bessel function of the second kind and Gamma function, respectively, and m_y and m_x are the two γ–γ distribution parameters related to the effective numbers of small- and large-scale scatterers in the OW link. In the strong turbulence regime, the channel response is accurately described by a negative-exponential pdf given by

$$f_{Z_i}(z) = \frac{L}{\overline{P}_{\text{in}}} \exp\left(-\frac{L\,z}{\overline{P}_{\text{in}}}\right). \tag{2}$$

The received optical signals traverse the corresponding amplifiers and receive a static gain equal to G. Apart from amplifying the signal, each amplifier generates noise through amplified spontaneous emission (ASE). The spectral density of the ASE noise is given by

$$P_n = n_{sp}\,h\,\frac{c}{\lambda}, \tag{3}$$

where c equals the speed of light in a vacuum, h is Planck's constant, n_{sp} is the population inversion factor in the amplifier and λ denotes the wavelength. The optical and noise signals beat on the PDs (square-law detectors) and a number of electrical noise components manifest at each PD output [8, 11]. The associated noise variances are denoted as thermal, shot, signal-spontaneous beating and spontaneous-spontaneous beating, respectively, and are calculated from

$$\sigma^2_{th} = \frac{4\,k_B\,T\,F_n\,B_e}{R_L}, \tag{4a}$$

$$\sigma^2_{shot}(Z_i) = 2\,q\,R\,\left(G\,Z_i + (G-1)\;P_n\,B_o\right)\;B_e, \tag{4b}$$

$$\sigma^2_{sig-sp}(Z_i) = 4\,R^2\,G\,Z_i\;(G-1)\;P_n\,B_e, \tag{4c}$$

and

$$\sigma^2_{sp-sp} = R^2\;\left((G-1)\;P_n\right)^2\;(2\,B_o - B_e)\,B_e, \tag{4d}$$

where B_o and B_e are the optical and electrical bandwidths, R is the photodiode responsivity, T is the receiver temperature, k_B denotes the Boltzmann constant, F_n is the electric noise figure and R_L is the resistor load. Given the noise variances in (4), the signal and noise powers for the '1' and '0' bits are calculated for each branch as

$$I_1(Z_i) = R\,G\,Z_i, \tag{5a}$$

$$\sigma^2_1(Z_i) = \sigma^2_{th} + \sigma^2_{shot}(Z_i) + \sigma^2_{sig-sp}(Z_i) + \sigma^2_{sp-sp}, \tag{5b}$$

and

$$I_0 = 0, \tag{6a}$$

$$\sigma^2_0 = \sigma^2_{th} + \sigma^2_{shot}(0) + \sigma^2_{sp-sp}, \tag{6b}$$

respectively. Typical values for the optical wireless channel, amplifier and receiver parameters are summarized in Tab. 1.

Tab. 1: System Parameters

Parameter	Symbol	Value
Number of branches	L	1-5
γ–γ parameter	m_x	5.93
γ–γ parameter	m_y	1.99
Amplifier gain	G	20 dB
Wavelength	λ	1550 nm
Population inversion factor	n_{sp}	4.0
Optical bandwidth	B_o	50 GHz
Photodiode responsivity	R	1.25 A/W
Receiver temperature	T	300^o K
Resistor load	R_L	100 Ω
Electrical noise figure	F_n	3 dB
Electrical bandwidth	B_e	7 GHz

3 Combiner Structures

3.1 Selection Combiner

The selection combiner samples all the received signals and selects the one with the highest power level, therefore

$$Z_{\rm sc} = \max_{i=1,2...L} \{Z_i\} . \tag{7}$$

An outage occurs when all the branches of the combiner simultaneously undergo a fade, and since the received signals are independent it follows that

$$\begin{aligned} P_{\rm out,sc} &= \prod_{i=1}^{L} \Pr\{BER(z_i) > BER_0\} \\ &= \Pr\{BER(z) > BER_0\}^L , \end{aligned} \tag{8}$$

where BER_0 is the desired BER level of the OWC system. Equivalently, one can calculate the outage probability from the receiver sensitivity $P_{\rm s,sc}$

$$P_{\rm out,sc} = \Pr\{z \le P_{\rm s,SC}\}^L = \left(\int_0^{P_{\rm s,sc}} f_Z(z)\, dz \right)^L . \tag{9}$$

The corresponding sensitivity is obtained after solving

$$\frac{1}{2} \operatorname{erfc}\left(\frac{Q(P_{\rm s,sc})}{\sqrt{2}} \right) = BER_0 , \tag{10}$$

where $\operatorname{erfc}(\cdot)$ denotes the complementary error function. The receiver Q-factor is given by

$$Q(z) = \frac{I_1(z)}{\sigma_0 + \sigma_1(z)} , \tag{11}$$

where it is assumed that each branch can safely estimate the channel state (channel-state information (CSI)-capable) and set its decision threshold to

$$I_{th}(z_i) = \frac{\sigma_0\, I_1(z_i)}{\sigma_0 + \sigma_1(z_i)} \tag{12}$$

on a bit-by-bit basis. The average BER can be calculated from the pdf of $Z_{\rm sc}$ as

$$\begin{aligned} \overline{BER}_{\rm sc} &= \int_0^{\infty} BER(z_{\rm sc})\, f_{Z_{\rm sc}}(z_{\rm sc})\, dz_{\rm sc} \\ &= \frac{1}{2} \int_0^{\infty} \operatorname{erfc}\left(\frac{Q(z_{\rm sc})}{\sqrt{2}} \right) f_{Z_{\rm sc}}(z_{\rm sc})\, dz_{\rm sc} , \end{aligned} \tag{13}$$

where $f_{Z_{\rm sc}}(z)$ is obtained by differentiating the cumulative distribution function of $Z_{\rm sc}$ from (9) and the result is

$$f_{Z_{\rm sc}}(z_{\rm sc}) = L \left(\int_0^{z_{\rm sc}} f_Z(z)\, dz \right)^{L-1} f_Z(z_{\rm sc}) . \tag{14}$$

3.2 Optimal and Equal Gain Combiners

The optimal combiner adds the received signals and noises after applying unequal gains w_i to branches. Assuming a CSI-capable combiner, the Q-factor is calculated from

$$Q_{\rm opt} = \frac{\sum_{i=1}^{L} w_i\, I_1(Z_i)}{\sqrt{\sum_{i=1}^{L} w_i^2\, \sigma_1^2(Z_i)} + \sqrt{\sum_{i=1}^{L} w_i^2\, \sigma_0^2}} . \tag{15}$$

The above equation can be written in a simpler form as

$$Q_{\rm opt} = Q_A \frac{\sum_{i=1}^{L} w_i Z_i}{\sqrt{\sum_{i=1}^{L} w_i^2\, (Z_i + Z_0)} + \sqrt{\sum_{i=1}^{L} w_i^2\, Z_0}} , \tag{16}$$

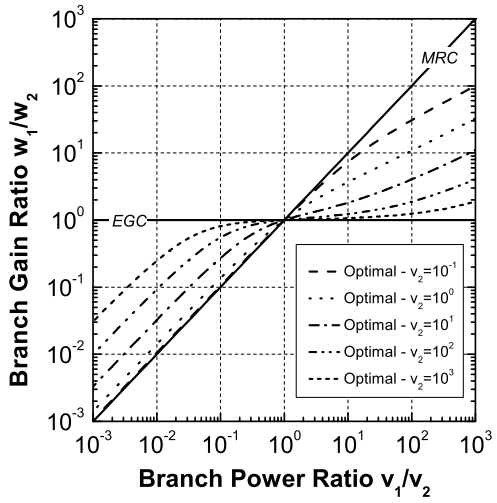

Fig. 2: Branch gain ratio $w_{1,\mathrm{opt}}/w_{2,\mathrm{opt}}$ as a function of the normalized branch powers $v_1 = Z_1/Z_0$ and $v_2 = Z_2/Z_0$ for a dual-branch optimal combiner arrangement.

where

$$Q_A = \frac{R\,G}{\sigma_A}\,, \tag{17a}$$

$$\sigma_A^2 = 2\,q\,R\,G\,B_e + 4\,R^2\,G\,(G-1)\,P_n\,B_e\,, \tag{17b}$$

$$Z_0 = \frac{\sigma_0^2}{\sigma_A^2}. \tag{17c}$$

We then find the the optimal gains after differentiating (16) with respect to the branch gains w_ℓ and the optimal gain values w_ℓ with $w_\ell, \ell = 1, 2, \ldots, L$ are calculated by numerically solving the following nonlinear set of equations

$$w_{\ell,\mathrm{opt}} \left(\frac{Z_\ell + Z_0}{\sqrt{\sum_{i=1}^{L} w_{i,\mathrm{opt}}^2\,(Z_i + Z_0)}} + \frac{Z_0}{\sqrt{Z_0 \sum_{i=1}^{L} w_{i,\mathrm{opt}}^2}} \right) = Z_\ell \frac{\sqrt{\sum_{i=1}^{L} w_{i,\mathrm{opt}}^2\,(Z_i + Z_0)} + \sqrt{Z_0 \sum_{i=1}^{L} w_{i,\mathrm{opt}}^2}}{\sum_{i=1}^{L} w_{i,\mathrm{opt}} Z_i}. \tag{18}$$

Some insights can be provided for $L = 2$ as presented in Fig. 2, where the branch gain ratio $w_{1,\mathrm{opt}}/w_{2,\mathrm{opt}}$ is plotted against the branch powers ratio Z_1/Z_2. The figure demonstrates that the optimal combiner operates in a fashion similar to an MRC when the input powers are low compared to Z_0 and the branch gain increases almost linearly with the input power. At higher input powers, however, the branch gain saturates and becomes relatively insensitive to further increases in power. In this regime, the branch gain is almost constant and the operation of the optimal combiner closely resembles the EGC one.

An upper limit for the Q-factor of the optimal combiner can be extracted by noting that

$$\sum_{i=1}^{L} w_i Z_i \le \sqrt{\sum_{i=1}^{L} w_i^2\,Z_i} \sqrt{\sum_{i=1}^{L} Z_i}\,, \tag{19a}$$

and

$$\sum_{i=1}^{L} w_i^2\,Z_i \le \sum_{i=1}^{L} w_i^2 \sum_{i=1}^{L} Z_i\,, \tag{19b}$$

yielding

$$Q_{\mathrm{opt}}\,(Z_s) \le \frac{R\,G}{\sigma_A} \left(\sqrt{Z_s + Z_0} - \sqrt{Z_0} \right), \tag{20}$$

where

$$Z_s = \sum_{i=1}^{L} Z_i \tag{21}$$

is a RV that is obtained from the sum of iid γ–γ or negative-exponential RVs. A closed form result for the pdf of Z_s is not known for γ–γ fading and it needs to be numerically calculated or approximated. In this work, we utilize the characteristic function of the γ–γ pdf to numerically calculate the pdf of Z_s using the Laplace and inverse Laplace transform pairs, i.e., $F_{Z_s}(\omega) = \mathcal{F}\{\omega;\ f_{Z_s}(z)\}$, and $f_{Z_s}(z) = \mathcal{F}^{-1}\{z;\ F_{Z_s}(\omega)\}$. For negative-exponential fading, Z_s follows the Erlang distri-

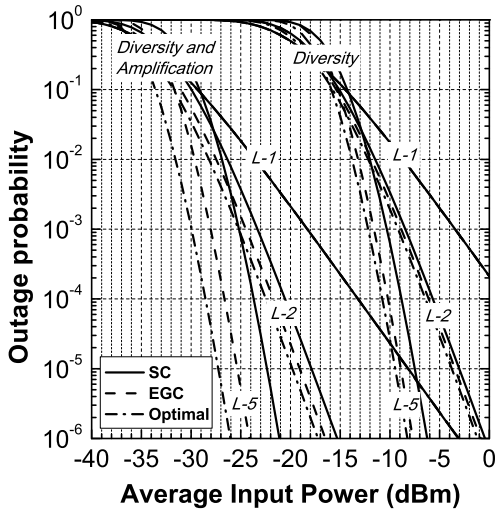

Fig. 3: Outage probability versus the average input power for γ–γ fading. The target BER equals $BER_0 = 10^{-3}$.

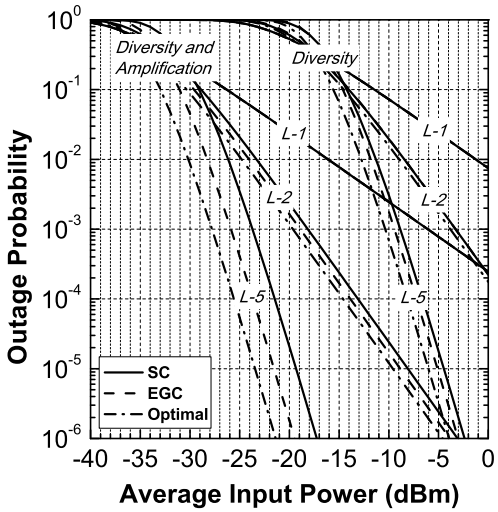

Fig. 4: Outage probability versus the average input power for negative-exponential fading. The target BER equals $BER_0 = 10^{-3}$.

bution

$$f_{Z_s}(z) = \left(\frac{L}{\overline{P}_{\rm in}}\right)^L \frac{z^{L-1}}{(L-1)!} \exp\left(-\frac{L\,z}{\overline{P}_{\rm in}}\right). \quad (22)$$

In comparison, the Q-factor of the EGC is calculated from (16) by applying equal gains

$$Q_{\rm egc}(Z) = Q_A\left(\sqrt{Z_s + L\,Z_0} - \sqrt{L\,Z_0}\right), \quad (23)$$

and the performance assessment of both combiners can be treated in a similar manner based on the statistics of RV Z_s.

We now focus on the derivation of the outage probability and the average BER of the optimal combiner. The outage probability at a required BER level BER_0 is calculated from

$$P_{\rm out,opt} \geq \Pr\left(z \leq P_{\rm s,opt}\right) = \int_0^{P_{\rm s,opt}} f_{Z_s}(z_s)\, dz_s, \quad (24)$$

where $P_{\rm s,opt}$ corresponds to the optimal combiner sensitivity

$$\frac{1}{2}\,{\rm erfc}\left(\frac{Q_{\rm opt}\left(P_{\rm s,opt}\right)}{\sqrt{2}}\right) = BER_0\,. \quad (25)$$

The average BER of the optimal combiner is also given by

$$\overline{BER}_{\rm opt} \geq \frac{1}{2}\int_0^{\infty} {\rm erfc}\left(\frac{Q_{\rm opt}(z)}{\sqrt{2}}\right) f_{Z_s}(z)\, dz\,. \quad (26)$$

Eqs. (24)–(26) are also valid for the EGC by replacing with the appropriate Q-factor expression.

4 Results and Discussion

4.1 Numerical Results

The performance of the proposed diversity setup with amplification is evaluated for a 10 Gb/s OWC link with channel, amplifier and receiver parameter values that are shown in Tab. 1. Figs. 3 and 4 illustrate the outage probability of the setup for $L = 1, 2$ and 5 diversity branches and a required BER of 10^{-3}. The outage probability of a non-amplified system is also plotted in the figure for benchmarking purposes. As it is shown in the figures, amplification and diversity both offer a significant improvement in the link budget, while the combination of the two methods amounts to a gain of over 25–30 dB depending

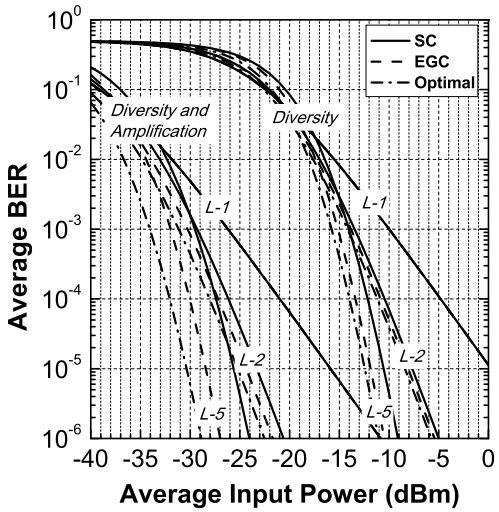

Fig. 5: Average BER versus the average input power for γ–γ fading.

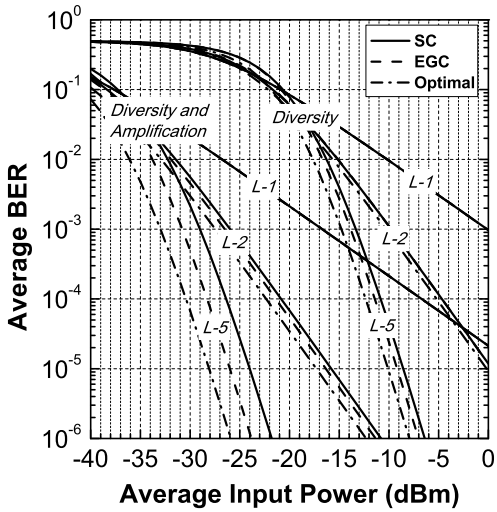

Fig. 6: Average BER versus the average input power for negative-exponential fading.

on the desired BER, the required outage probability and the number of branches at the receiver. The results also show that the EGC outperforms the SC by 3 dB in γ–γ fading and 2 dB in negative-exponential fading. Similar performance is observed in the average BER plots of Figs. 5 and 6, where link margins of the same value are achieved for the diversity system with pre-amplification. Finally, the results suggest the optimal combiner can potentially provide an additional link gain of up to 2 dB in both fading environments. Since this result is based upon an approximation in (24) and (26), we further investigate the optimal combiner performance via simulation.

4.2 Simulation Results

The performance of the proposed optimal combiner was Monte-Carlo simulated for both γ–γ and negative-exponential fading. For comparison purposes, SC and EGC structures were also also simulated under the same conditions. The performance of the SC and EGC was utilized to verify the validity of the simulator, since the simulation results can be easily cross-checked against the analytical relations presented earlier, and no discrepancy between theoretical and simulation results was observed. Finally, the MRC was also included in the simulation so as to compare the optimal combiner with all popular combiner structures, despite the fact that it is not possible to analytically assess the MRC performance for the case of diversity reception with amplification.

The average BER simulation results against the average input power for SC, EGC, MRC and optimal combining schemes for $\gamma - \gamma$ and negative-exponential fading are shown in Fig. 7 for $L = 5$ branches. The results show that the optimal combiner performs only marginally better than the MRC, with the EGC being slightly worse and introducing a power penalty of less than 0.5 dB. These results are plotted for the parameters summarized in Tab. 1 and correspond to a relative noise parameter $Z_0 = 22$ nW, which in turn means that the receiver suffers from significant ASE and thermal noise as compared to the amplified signal. Following Fig. 2, the optimal combiner gains are close to MRC for the high noise regime, thus an almost identical performance for the two observed.

To further explore this result, a second, lower relative noise, simulation scenario was investigated. In this second scenario, the amplifier gain was increased to 30 dB so as to limit the effect of the thermal noise, while at the same

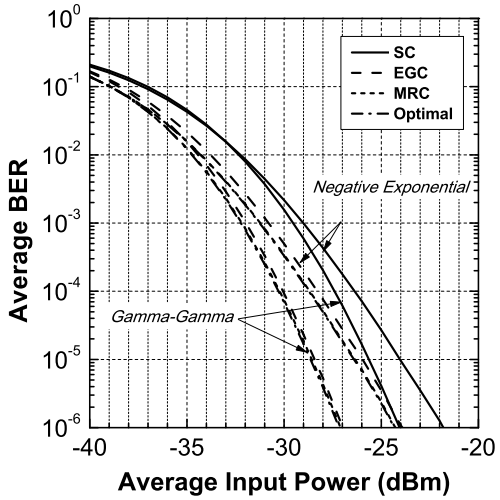

Fig. 7: Simulated average BER for a high relative noise parameter z_0 against the average input power for for SC, EGC, MRC and optimal combining schemes for gamma-gamma and negative exponential fading.

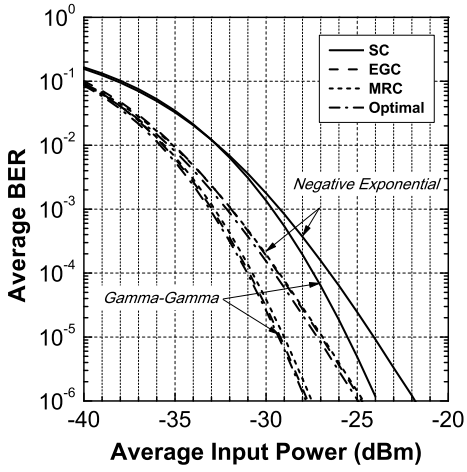

Fig. 8: Simulated average BER for a lower relative noise parameter Z_0 against the average input power for for SC, EGC, MRC and optimal combining schemes for gamma-gamma and negative exponential fading.

time narrower optical filters were utilized ($B_o = 20$ GHz and $B_e = 10$ GHz, respectively), reducing the relative noise parameter to $Z_0 = 4$ nW. The results are presented in Fig. 8, where it can be verified that the optimal combiner performs closer to the EGC, while the MRC introduces a limited power penalty.

The simulation results verify the dual operation of the optimal combiner that is dependent on the system noise (optical and thermal), as predicted by the presented theory. From a practical perspective, the optimal combiner can be approximated by maintaining the most significant terms of (18) to obtain the simplified gain, which is given as

$$w_{\ell,\mathrm{opt}} = \frac{Z_\ell}{Z_\ell + Z_0}\,. \tag{27}$$

Depending on the noise conditions, the optimal combiner will either provide the MRC gains

$$w_{\ell,\mathrm{opt}} = \frac{Z_\ell}{Z_0}\,, \tag{28}$$

whenever $Z_\ell \ll Z_0$, or the EGC gains

$$w_{\ell,\mathrm{opt}} = 1\,, \tag{29}$$

whenever $Z_\ell \gg Z_0$. It should be noted that this approximation does not add any significant complexity with respect to the MRC, since both combiners require the estimation of the OW channel. If the exact (18) is utilized, an additional computational effort must be made to solve the L non-linear equations.

5 Conclusion

We have presented a mathematical description of the outage probability and the average BER for pre-amplified OWC systems that optimally combine signals from multiple receivers. Based on the mathematical model, we derived results on an electronic combiner that optimizes the BER performance of the system under medium and strong fading condition. The analytical results show that the optimal combiner performs similar to the EGC for increased signal powers, while its per-branch operation reverts to the MRC in the presence of fade. Simulation results verified the presented analysis, but also predicted that the optimal combiner provides a limited link budget gain compared to EGC and MRC.

Acknowledgment

This work was funded by COST Action IC1101 "Optical Wireless Communications–An Emerging Technology".

References

[1] Abtahi, M., Lemieux, P., Mathlouthi, W., Rusch, L.A. (2006). Suppression of turbulence-induced scintillation in free-space optical communication systems using saturated optical amplifiers. 24(12), 4966–4973

[2] Andrews, L.C., Phillips, R.L. (2005). *Laser beam propagation through random media*. SPIE Press, Bellingham, Washington, 2 edition

[3] Anguita, A., Neifeld, M.A., Hildner, B., Vasic, B. (2010). Rateless coding on experimental temporally correlated FSO channels. 28(7):990–1002

[4] Barakat, R. (Aug 1988). Level-crossing statistics of aperture-integrated isotropic speckle. *J. Opt. Soc. Am. A*, 5(8), 1244–1247

[5] Bayaki, E., Schober, R., Michalopoulos, D.S. (2012). EDFA-based all-optical relaying in free-space optical systems. 60(12):3797–3807

[6] Datsikas, C.K., Peppas, K.P., Sagias, N.C., Tombras, G.S. (2010). Serial free-space optical relaying communications over gamma-gamma atmospheric turbulence channels. *IEEE/OSA Journal of Optical Communications and Networking*, 2(8):576–586

[7] Hulea, M., Ghassemlooy, Z., Rajbhandari, S., Tang, X. (2014). Compensating for optical beam scattering and wandering in FSO communications. 32(7):1323–1328

[8] Humblet, P.A., Azizoglu, M. (1991). On the bit error rate of lightwave systems with optical amplifiers. 9(11):1576–1582

[9] Khalighi, M.-A., Schwartz, N., Aitamer, N., Bourennane, S. (2009). Fading reduction by aperture averaging and spatial diversity in optical wireless systems. *IEEE/OSA Journal of Optical Networking*, 1(6):580–593

[10] Navidpour, S.M., Uysal, M., Kavehrad, M. (2007). BER performance of free-space optical transmission with spatial diversity. 6(8):2813–2819

[11] Olsson, N.A. (1989). Lightwave systems with optical amplifiers. 7(7):1071–1082

[12] Peppas, K.P., Lazarakis, F., Alexandridis, A., Dangakis, K.. (2012). Simple, accurate formula for the average bit error probability of multiple-input multiple-output free-space optical links over negative exponential turbulence channels. *Opt. Lett.*, 37(15):3243–3245

[13] Polishuk, A., Arnon, S. (2004). Optimization of a laser satellite communication system with an optical preamplifier. *J. Opt. Soc. Am. A*, 21(7):1307–1315

[14] Popoola, W.O., Ghassemlooy, Z. (2009). BPSK subcarrier intensity modulated free-space optical communications in atmospheric turbulence. 27(8):967–973

[15] Razavi, M., Shapiro, J.H. (2005). Wireless optical communications via diversity reception and optical preamplification. 4(3):975–983

[16] Safari, M., Uysal, M. (2008). Relay-assisted free-space optical communication. 7(12):5441–5449

[17] Uysal, M., Li, J., Yu, M. (2006). Error rate performance analysis of coded free-space optical links over gamma-gamma atmospheric turbulence channels. 5(6):1229–1233

[18] Strömqvist Vetelino, F., Young, C., Andrews, L., Recolons, J. (2007). Aperture averaging effects

on the probability density of irradiance fluctuations in moderate-to-strong turbulence. *Appl. Opt.*, 46(11):2099–2108

[19] Wilson, S.G., Brandt-Pearce, M., Cao, Q., Baedke, M. (2005). Optical repetition MIMO transmission with multi-pulse PPM. 23(9):1901–1910

[20] Xu, F., Khalighi, A., Caussé, P., Bourennane, S. (2009). Channel coding and time-diversity for optical wireless links. *Opt. Express*, 17(2):872–887

[21] Yiannopoulos, K., Sagias, N., Boucouvalas, A.C., Uysal, M., Ghassemlooy, Z. (2016). Optimal combiners in optical wireless systems with spatial diversity and pre-amplification. In *Communications (ICC), 2016 IEEE International Conference on*

[22] Zhao, W., Han, Y., Yi, X. (2013). Error performance analysis for fso systems with diversity reception and optical preamplification over gamma–gamma atmospheric turbulence channels. *Journal of Modern Optics*, 60(13):1060–1068

[23] Zhu, X., Kahn, J.M. (2003). Performance bounds for coded free-space optical communications through atmospheric turbulence channels. 51(8):1233–1239